JEE Journal of Ecological Engineering

Journal of Ecological Engineering, 2026, 27(9), 461–472
https://doi.org/10.12911/22998993/221724
ISSN 2299–8993, License CC-BY 4.0

Received: 2026.04.29
Accepted: 2026.07.15
Published: 2026.08.01

Factorial design-assisted electrochemical determination of azithromycin in the presence of coexisting antibiotics

Sadik Cenolli[1,2*], Majlinda Vasjari[1,2], Nevila Broli[1,2], Ana Ameda[1,2], Lueda Kulla[1,2], Besnik Baraj[1,2]

[1] Faculty of Natural Sciences, University of Tirana, 1001 Tirana, Albania
[2] NanoBalkan, Academy of Sciences of Albania, 1001 Tirana, Albania
* Corresponding author's e-mail: sadik.cenolli@fshn.edu.al

ABSTRACT

Antibiotics are among the most widely used pharmaceuticals, and their indiscriminate application has raised significant environmental and public health concerns. Rapid and cost-effective detection of antibiotic residues in surface water remains a major analytical challenge. However, limited studies have investigated the combined influence of multiple antibiotics on electrochemical signals during simultaneous detection. This study aims to evaluate the effects and interactions of azithromycin (AZI), tetracycline (TET), ampicillin (AMPIC), and penicillin (PEN) using factorial analysis while minimizing the number of required experiments. Electrochemical measurements were performed using square wave voltammetry (SWV) with a ZnO nanoparticle-modified carbon paste electrode under optimized conditions for AZI detection (potential range 0–1.5 V, amplitude 50 mV, step potential 5 mV, and frequency 15 Hz). The sensor exhibited a linear response in the range of 10–109 µM, with a limit of detection (LOD) of 3.22 µM and a limit of quantification (LOQ) of 9.77 µM. The factorial model showed strong agreement between predicted and experimental values and revealed that AMPIC significantly enhanced the AZI current signal, while interactions among antibiotics had moderate effects. In this work, factorial analysis was integrated with ZnO-modified electrochemical sensing to investigate the interactions of antibiotics with multiple analytes, and the findings demonstrate the potential of this approach for optimizing electrochemical detection methods in complex environmental matrices.

Keywords: ZnO nanoparticles, carbon paste electrode, antibiotics, interaction.

INTRODUCTION

Antibiotics have revolutionized modern medicine by effectively combating bacterial infections. However, their extensive and often uncontrolled use has led to growing environmental and public health concerns. Residues from human and veterinary applications frequently reach aquatic environments through wastewater discharge, agricultural runoff, and improper disposal of pharmaceuticals (Mishra et al., 2023; Cherian et al., 2023; Kumar et al., 2018; Mohd Noor et al., 2023; Muaz et al., 2018). The persistence of antibiotic residues in surface waters contributes to the development of antimicrobial resistance, disrupts aquatic ecosystems, and poses long-term health risks to humans and wildlife (Schar et al., 2020; Cabello, 2006; Okocha et al., 2018; Awad et al., 2013). Conventional detection methods such as mass spectrometry, high-performance liquid chromatography (HPLC), and capillary electrophoresis as Sun et al., (2018) and Souza et al., (2005) report, provide high sensitivity and accuracy but they are costly, time-intensive, and require elaborate sample preparation (Wang et al., 2024; Wang et al., 2022; Wang et al., 2019; Fabregat-Safont et al., 2023). In contrast, electrochemical methods—including voltammetry and amperometry—offer attractive alternatives due to their simplicity, low cost, rapid response, and potential for on-site environmental monitoring (Nguyen et al., 2023; Lowdon et al., 2020; Tavares et al., 2021; Pan et al., 2021; Hu et al., 2018; Peng et al., 2011; Ensafi et al., 2013; Vajdle et al., 2017; Liu et al., 2022; Zokhtareh et al., 2023). Despite these advantages, simultaneous detection of multiple antibiotics

remains challenging due to overlapping signals, interferences, and matrix effects. Traditional univariate optimization approaches (where a one factor varied at a time), fail to address these complexities, as interactions between analytes can significantly alter electrochemical responses. Factorial design provides a systematic and statistically robust framework for studying the effects of multiple variables and their interactions simultaneously (Shrestha, 2021; (Tavakol and Wetzel, 2020). This approach not only reduces the number of experiments but also enhances predictive power, enabling a more accurate understanding of signal variations (Bentler and Leeuw, 2011).

In this work, we applied factorial analysis to evaluate the influence of four commonly used antibiotics in Albania—Azithromycin (AZI), Tetracycline (TET), Ampicillin (AMPIC), and Penicillin (PEN)—on electrochemical detection signals, under optimized conditions for AZI (Machowska and Lundborg, 2018; Bruyndonckx et al., 2021; Hoxha et al., 2015; Mihani and Këlliçi, 2018; Mohan and Renjanadevi, 2016; Bozo et al., 2024). It was hypothesized that the coexistence of these antibiotics could significantly influence the electrochemical signal through interaction effects, which can be effectively identified using factorial analysis.

Therefore, the aim of this study was to evaluate the individual and combined effects of AZI, TET, AMPIC, and PEN on the electrochemical response using factorial analysis and a ZnO nanoparticle-modified carbon paste electrode, to optimize simultaneous antibiotic detection and establish a predictive mathematical model for complex aqueous matrices. By integrating electrochemical techniques with factorial design, this study provides a novel and cost-effective framework for reliable monitoring of antibiotic contamination in aquatic environments.

MATERIALS AND METHODS

Reagents and materials

All chemicals that are used were of analytical grade and without further purification. So*l*utions were prepared with double-distilled, deionized water. Azithromycin, penicillin, ampicillin and tetracycline (>98%) were obtained from Sigma-Aldrich. Antibiotics stock solutions freshly prepared in ethanol (>99.5%, Sigma-Aldrich), acetate buffer or bi-distillate water. Acetate buffer (0.1 M, pH~5) prepared from sodium acetate and acetic acid. Graphite powder with particle size 71–90 μm and purity 99.9% was obtained from Alfa Aesar (Thermo Fisher Scientific, USA). Paraffin oil was provided by Zeta Farmaceutici (Dolo, Italy). All other reagents: sodium nitrate, sulfuric acid (99%), potassium permanganate, hydrogen peroxide (30%), hydrochloric acid (37%), nickel sulfate, zinc sulfate heptahydrate, trisodium citrate dehydrate and potassium ferrocyanide/potassium ferricyanide were provided from Merck (KGaA, Darmstadt, Germany). For electrochemical measurements a PalmSens 4 potentiostat/galvanostat is used in a three-electrode system with a platinum counter electrode, an Ag/AgCl reference electrode, and a carbon paste un/modified as working electrode. Square-wave voltammetry (SWV) was employed under the following conditions: potential range 0–1.5 V, frequency 15 Hz, step potential 5 mV, amplitude 50 mV, equilibration time 10 s.

Synthesis of ZnO nanoparticles

ZnO nanoparticles were s*y*nthesized via a precipitation method (Kołodziejczak-Radzimska and Jesionowski, 2014; Patil VB et al., 2022). Briefly, zinc sulfate heptahydrate $ZnSO_4 \cdot 7H_2O$ and trisodium citrate dihydrate $Na_3C_6H_5O_7 \cdot 2H_2O$ were dissolved in double-distilled water. Subsequently, NaOH was added, and the mixture was stirred for 2 h. The r*e*sulting suspension was centrifuged at 10,000 rpm for 5 min, washed several times with distilled water, and dried at 60 °C for 12 h (Zaaba et al., 2017).

Synthesis of GO modifier

Graphene oxide (GO) was prepared using a mod*i*fied Hummer's method (Choi, et al., 2010; Sulciute et al., 2021). Graphene, sodium n*i*trate $NaNO_3$ and concentrated H_2SO_4 were mixed under continuous stirring until homogenization was achieved. The reaction mixture was cooled in an ice bath for 15 min, after which $KMnO_4$ was gradually added with constant stirring. The suspension was maintained under magnetic stirring at room temperature for 1 h, followed by the addition of 100 mL of distilled water in an ice bath. The mixture was subsequently heated at >90 °C for 1 h, after which of distilled water and 30% H_2O_2 were introduced. The resulting dispersion was subjected to ultra-sonication for 30 min at 25 °C.

Modified CPE preparation

Different types of modified carbon pastes were prepared and compared with each other for their behavior towards AZI additions. Carbon paste modified with GO (CPE_GO) is prepared by 1 g of carbon powder that is homogenized for 1 h in a mortar with 0.1 g GO and 0.3 mL paraffin and then is packaged in a syringe. Carbon paste modified with ZnO (CPE_ZnO) (Novakovic et al., 2025; Patil et al., 2022; Pogăcean et al. 2022) is prepared by 1 g of carbon powder that is homogenized for 1 h in a mortar with 0.1 g ZnO nps and 0.3 mL paraffin and then is packaged in a syringe. Carbon paste modified with GO and ZnO (CPE_GO@ZnO) is prepared by 2 g of carbon powder that is homogenized for 1 h in a mortar with 0.1 g GO, 0.1 g ZnO nps and 0.6 mL paraffin and then is packaged in a syringe (Belcovici et al., 2023). All electrodes were stored a*t* room temperature and mechanically polished before use.

Synthetic matrices preparation

The composition of synthetic samples was selected based on a full factorial experimental design (2^4). With four independent factors, a total of 16 experimental runs ($2^4 = 16$) were prepared to evaluate both individual and interaction effects. The relationship between the measured electrochemical signal (current, I) and the independent variables was modeled using a polynomial factorial model including main, interaction, and higher-order terms. The statistical modeling and data analysis were performed using Python programming language, employing standard scientific libraries for regression and factorial analysis

A second-order factorial model was considered sufficient to describe the system, assuming that higher-order interactions are negligible compared to main and two-factor interaction effects. Four factors corresponding to four antibiotics were investigated under optimized conditions: X_1 – AZI; X_2 – TET; X_3 – AMPIC; X_4 – PEN. The two concentration levels: 5 µM (low, −) and 20 µM (high, +) selected were chosen based on preliminary calibration experiments to ensure operation within the linear response range of the sensor and to provide sufficient signal variation for factorial analysis. Additionally, all tested concentrations were above the limit of detection, ensuring reliable electrochemical quantification (Table 1).

Measurements developed in an electrochemical cell that contain 15 mL of 0.1 M acetate buffer with pH~ 5. All measurements are performed using the SWV technique under the following conditions t_{eq} = 10 s, E_{beg} = 0 V, E_{end} =1.5 V, E_{step} = 5 mV, Amplitude =50 mV, frequency =10 Hz, optimized condition for AZI detection.

RESULTS AND DISCUSSIONS

Morphological characterization of CPE

By scanning electron microscopy (SEM) at different magnifications, the morphology of the ZnO-modified carbon paste electrode (CPE_ZnO) was examined while the elemental composition was analyzed using energy-dispersive X-ray spectroscopy (EDX).

The low-magnification SEM image (Figure 1) displays a rough and granular surface structure typical of carbon paste, indicating the presence of ZnO nanoparticles uniformly embedded within the carbon matrix. At higher magnification, ZnO nanostructures appear as agglomerated, flower-like formations composed of fine, nanosized

$$I = \sum_{i=0}^{i=n} a_i X_i + \sum_{\substack{i,j=1 \\ i \le j}}^{n} a_{ij} X_i X_j + \sum_{\substack{i,j,k=1 \\ i \le j \le k}}^{n} a_{ijk} X_i X_j X_k + \sum_{\substack{i,j,k,l=1 \\ i \le j \le k \le l}}^{n} a_{ijkl} X_i X_j X_k X_l + \cdots \quad (1)$$

Table 1. Summary of planned experiments

Experiment	1	2	3	4	5	6	7	8	9	10	11	12	13	14	15	16
F1≡AZI	-	+	-	+	-	+	-	+	-	+	-	+	-	+	-	+
F2≡TET	-	-	+	+	-	-	+	+	-	-	+	+	-	-	+	+
F3≡AMPIC	-	-	-	-	+	+	+	+	-	-	-	-	+	+	+	+
F4≡PEN	-	-	-	-	-	-	-	-	+	+	+	+	+	+	+	+

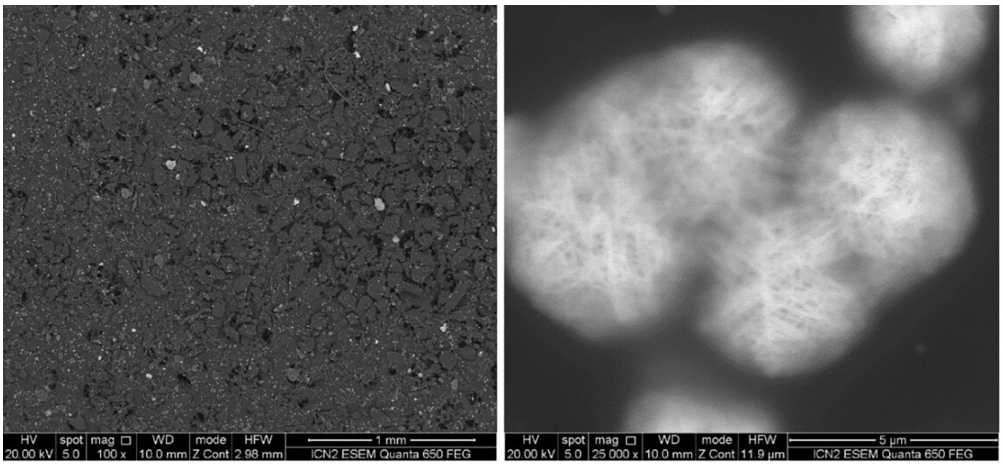

Figure 1. SEM in different magnification, for the CPE modified with ZnO

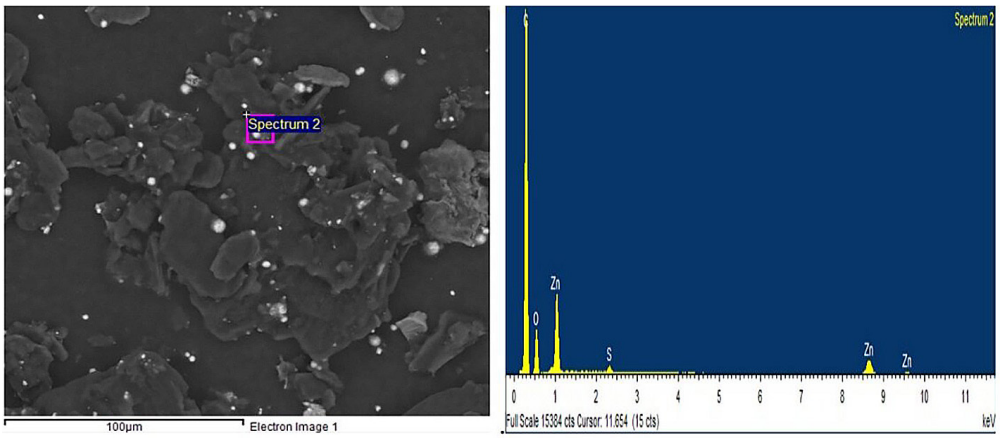

Figure 2. EDX spectrum of the CPE modified with ZnO

rods, confirming the nanometric character of the modifier. The observed morphology suggests that ZnO nanoparticles increase surface heterogeneity, which is expected to enhance the density of electroactive sites and improve electron transfer kinetics. The EDX spectrum (Figure 2) confirms the elemental composition of the modified surface, revealing characteristic peaks corresponding to zinc and oxygen, along with carbon from the paste matrix. The homogeneous distribution of Zn and O signals further confirms successful incorporation of ZnO nanoparticles.

Electrochemical properties of electrode

In 5 mM $[Fe(CN)_6]^{4-}/[Fe(CN)_6]^{3-}$ solution, was performed the electrochemical characterization of unmodified and modified electrodes using the cyclic voltammograms recorded obtained using bare CPE, CPE_GO, CPE_ZnO and CPE_GO@ZnO (Figure 3). The cyclic voltammograms reveal clear differences in the electrochemical behavior of the modified electrodes. The bare CPE exhibits relatively low current response with a more rectangular shape, indicating predominantly capacitive behavior and limited redox activity. Upon modification with graphene oxide (CPE_GO), a noticeable increase in current is observed, suggesting improved conductivity and enhanced electron transfer. The CPE_ZnO electrode shows the highest anodic and cathodic peak currents, demonstrating superior electrochemical activity and indicating that ZnO significantly facilitates redox processes. Furthermore, the CPE_GO@ZnO composite displays enhanced performance compared to CPE and CPE_GO, confirming a synergistic effect between graphene oxide and ZnO that improves both conductivity and active surface area. Overall, the peak separation observed in all voltammograms suggests quasi-reversible electrochemical behavior, with the modified electrodes, particularly CPE_ZnO and CPE_GO@ZnO, exhibiting improved electron transfer kinetics.

Electrochemical performance and electroactive surface area evaluation

Cyclic voltammetry (CV) measurements were carried out for electrochemical characterization, in a potassium ferricyanide solution using bare CPE, CPE_GO, CPE_ZnO, and CPE_GO@ZnO electrodes. The redox probe interacts with the electrode surfaces, enabling electron transfer through surface adsorption and for this reason all electrodes exhibited quasi-reversible redox behavior, as evidenced by the separation between anodic and cathodic peaks. The peak-to-peak potential separation (ΔEp) was estimated to be approximately 750 mV for CPE, 500 mV for CPE_GO, 300 mV for CPE_GO@ZnO, and 170 mV for CPE_ZnO. The bare CPE showed the largest ΔEp along with the lowest current response, indicating slow electron transfer kinetics. Upon modification with GO (CPE_GO), ΔEp decreased and the peak currents increased, suggesting improved conductivity. The CPE_ZnO electrode exhibited the smallest ΔEp and the highest peak currents, reflecting faster electron transfer and enhanced electrochemical activity. Meanwhile, the CPE_GO@ZnO electrode displayed intermediate behavior, with improved performance compared to CPE_GO but not exceeding that of CPE_ZnO. This suggests that ZnO plays the dominant role in enhancing the electrochemical response, while the addition of GO does not provide significant further improvement under these conditions.

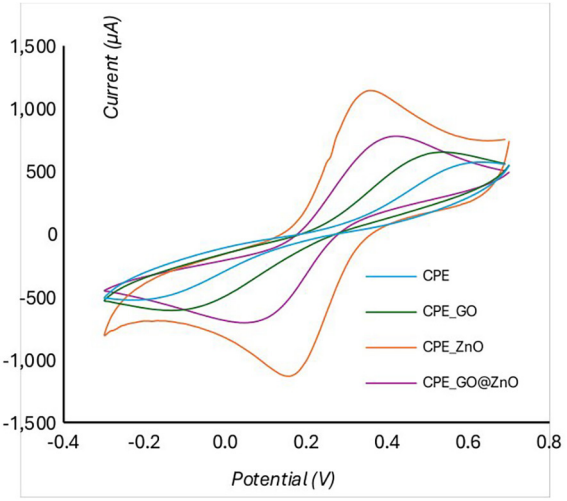

Figure 3. Voltammograms of CV (E=0.7: -0.3 V, E_{step} = 0.01 V, scan rate= 0.1 v/s) for unmodified and modified CPE in 5 mM $[Fe(CN)_6]^{4-}/[Fe(CN)_6]^{3-}$

Using the double-layer capacitance C_{dI} method, in 0.1 M acetate buffer (pH ~ 5) was evaluated the electrochemically active surface area (ECSA) of CPE, CPE_GO, CPE_ZnO, and CPE_GO@ZnO electrodes. In Figure 4 (A-D) shows the

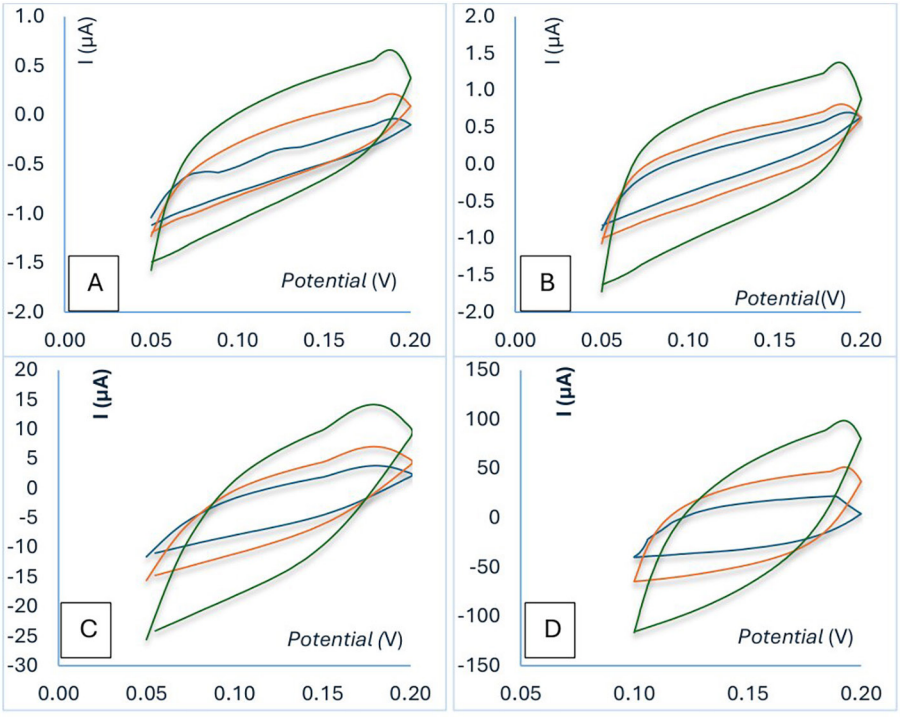

Figure 4. CVs of: A) CPE, B) CPE_GO, C) CPE_GO@ZnO, D) CPE_ZnO; with scan rate 10 mV/s (blue), 20 mV/s (red) and 50 mV/s (green) recorded in 0.1 M acetate, pH ~ 5

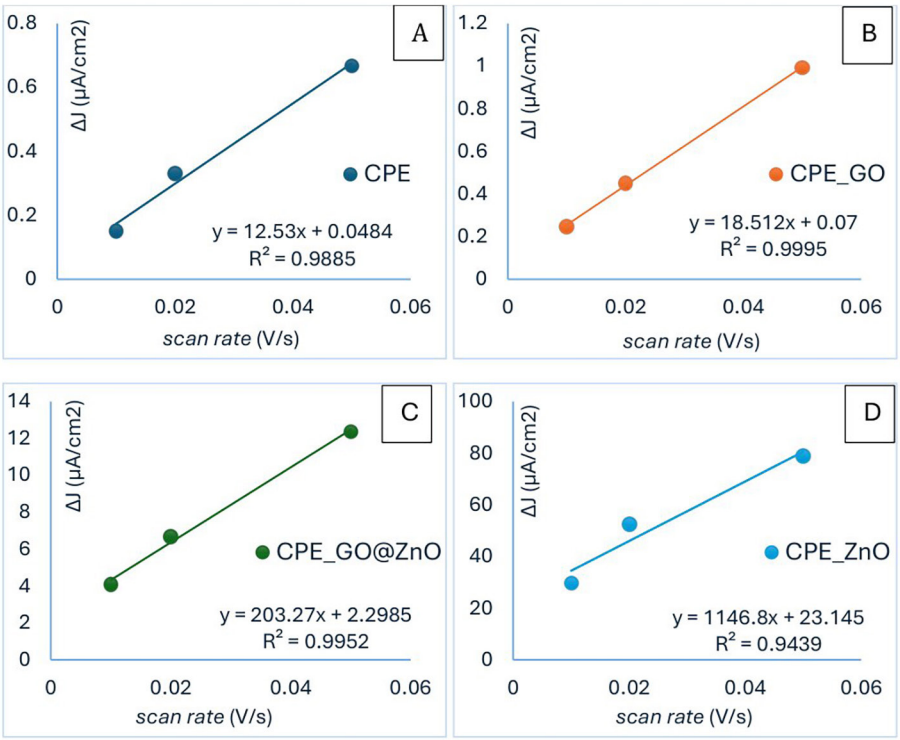

Figure 5. Relation of average current density ($\Delta j = (j_a - j_c)/2$) with scan rate from the corresponding CVs A) CPE, B) CPE_GO, C) CPE_GO@ZnO, D) CPE_ZnO; recorded in 0.1 M acetate, pH ~ 5

voltammograms of CV recorded in this media for all electrodes in three scan rates levels 10, 20 and 50 mV/s.

In the non-Faradaic region, as shown in Figure 5, CdI values were calculated from the slope of the current density (μA/cm²) versus scan rate (V/s) relationship. Table 2 summarizing the electrochemically active surface area (ECSA), using a specific capacitance of C_s = 30 μA/cm² (Yadav et al., 2018) and the roughness factor (RF = ECSA / S_g, S_g=0.785 cm²) for each electrode:

Electrochemical behavior of AZI

Analytical performance of the CPE modified for AZI determination is studied using SWV under the optimized parameters and three electrode system: CPE_ZnO as working electrode, Ag/AgCl/ Cl- as reference electrode and Pt as a counter electrode. The additions of standards solution of AZI are applied in 15 mL of 0.1 M acetate buffer and pH~ 5. The voltammograms are shown in Figure 6 for the CPE_ZnO sensor.

Considering three independent replicates, were determined the analytical performance parameters within the l*i*near range of the calibration plots for the various CPE@modifier electrodes. The CPE_ZnO electrode exhibited a good linear response over a concentration range of 10–109 μM, demonstrating good analytical applicability within this interval. A high sensitivity of 512 μA/mM was obtained, indicating a strong current response to changes in analyte concentration. The calibration curve exhibited excellent linearity, with a correlation coefficient R^2 = 0.9974, confirming the reliability and reproducibility of the analytical response. The limit of detection (LoD) and limit of quantification (LoQ) were calculated (3.22 μM and 9.77 μM, respectively) and indicating the high sensitivity of the electrode toward low analyte concentrations and its suitability for accurate detection and quantification.

Table 2. Summary of ECSA for different types of carbon electrodes

Electrode	CPE	CPE_GO	CPE_GO@ZnO	CPE_ZnO
ECSA (cm²)	0.418	0.617	6.78	38.2
R.F	0.532	0.786	8.31	48.7

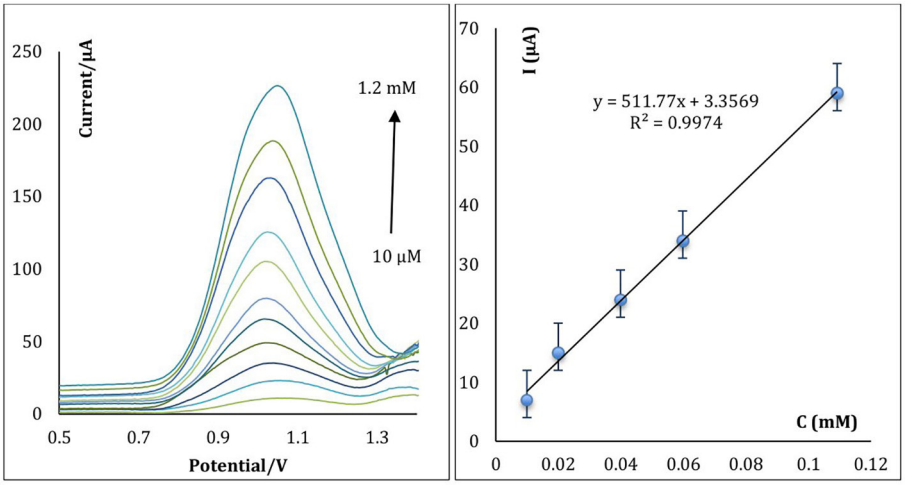

Figure 6 Voltammograms of SWV (E= 0–1.5 V, equilibration time 10s, frequency 15 Hz, Amplitude 50 mV, step potential 5 mV) for addition of AZI 10–1.2 mM in acetate buffer pH ~5, for CPE_ZnO and calibration curve for the liner range 10–109 µM AZI

Interference from foreign ions

In practical applications, the selectivity of the CPE_ZnO sensor was evaluated using SWV (E= 0–1.5 V, equilibration time 10 s, amplitude 50 mV, step potential 5 mV, frequency 15 Hz) in presence of some of the common ions (Pb^{2+}, Cu^{2+}, Fe^{3+} etc.) in a constant concentration of 50 µM AZI. Relative current change (%) were calculated as ration of each ion current and AZI current and as shown in the Figure 7, these species include minor changes in the AZI peak current, demonstrating in this case, a good selectivity of this sensor for AZI determination.

As the relative signal variations ranged from 93% to 107%, these changes may be attributed to catalytic effects, complexation phenomena, or partial inhibition of the electrochemical process. Such variations likely reflect the combined influence of surface interactions at the modified electrode interface and the dynamic behavior of the analytes under the studied conditions (Kulla et al., in press; Ameda et al., in press), indicating a complex interplay between electrochemical activity and molecular interactions within the sensing system.

Study of reproducibility, repeatability, and stability

The analytical performance of the CPE_ZnO sensor for AZI detection was assessed in terms of repeatability, stability, and reproducibility. Repeatability tests performed through three

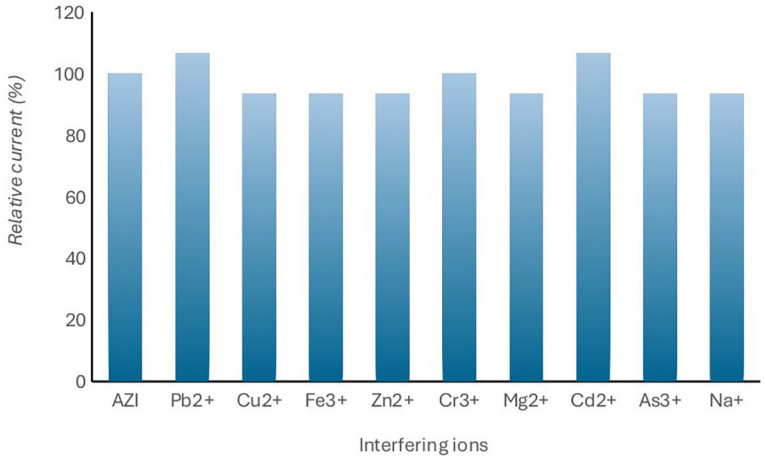

Figure 7. Relative current (%) response of the CPE_ZnO electrode recorded for 50 µM AZI in the presence of selected potential interfering ions

successive measurements of a 10 µM standard solution resulted in a relative standard deviation (RSD) of 5.4%, indicating very good consistency of the electro-sensor response. The sensor stability was assessed after one week of storage under ambient laboratory conditions, and it maintained 94% of its initial response, confirming satisfactory long-term stability and good signal retention over time. Furthermore, reproducibility was evaluated through five independent measurements, yielding an RSD of 3.2%, which highlights the excellent reliability and precision of the electrode for AZI detection.

Matrix analyses

After optimizing the experimental conditions for the electrochemical determination of AZI—such as the type of modifier used in the CPE electrodes, the choice of buffer and its pH, as well as the electrochemical technique and its operating parameters—16 different solutions with defined antibiotic concentrations were prepared according to the work plan described above. The corresponding peak intensities were then recorded. The Table 3 below presents data from selected experiments, along with the observed peaks and their respective voltammograms shows in Figure 8.

Electrochemical measurements from the 16 factorial experiments revealed distinct influences of individual antibiotics and their interactions on the AZI signal. A regression model was constructed using coded variables, which strongly agreed with experimental data:

$$I = 2.8456 \times F1 + 0.1331 \times F2 + 0.9426 \times F3 + 0.1234 \times F4 - 1.0535 \times F1 \times F2 - 0.4025 \times F1 \times F3 + 0.3537 \times F1 \times F4 - 0.3723 \times F2 \times F3 - 0.4568 \times F2 \times F4 - 0.5198 \times F3 \times F4 + 1.2226 \times F1 \times F2 \times F3 - 0.0309 \times F1 \times F2 \times F4 + 0.3726 \times F1 \times F3 \times F4 + 0.63694 \times F2 \times F3 \times F4 + 0.7857 \times F1 \times F2 \times F3 \times F4 + 8.4092 \quad (2)$$

Then this equation is transformed into real variables:

$$I^* = 0.71874 \times AZI + 0.62838 \times TET + 0.75509 \times AMPIC + 0.03234 \times PEN - 0.01524 \times AZI \times TET - 0.01562 \times AZI \times AMPIC + 0.03496 \times AZI \times PEN - 0.02292 \times TET \times AMPIC + 0.01272 \times TET \times PEN - 0.00035 \times AMPIC \times PEN - 0.00021 \times AZI \times TET \times AMPIC - 0.00318 \times AZI \times TET \times PEN - 0.00222 \times AZI \times AMPIC \times PEN - 0.00159 \times TET \times AMPIC \times PEN + 0.00025 \times AZI \times TET \times AMIPC \times PEN - 9.26928 \quad (3)$$

The strong concordance between the values predicted by the equation with real variables and those obtained experimentally permits a detailed assessment of the individual effects of each antibiotic on the analytical signal of AZI, as well as the influence of their mutual interactions on this response. Factors separately have a positive influence, "AMPIC" is the biggest and "PEN" is

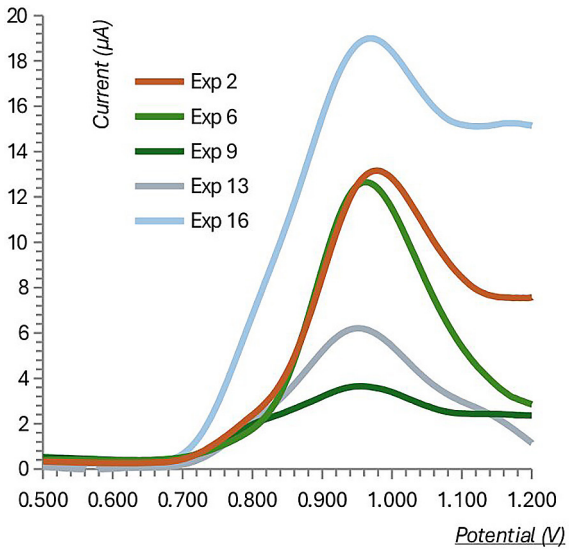

Figure 8. Voltammograms of SWV (E= 0-1.5 V, equilibration time 10s, step potential 5 mV, Amplitude 50 mV, frequency 15 Hz) in 0.1 M acetate buffer pH~5, with CPE_ZnO for addition of antibiotics, according to planned experiment

Table 3. The data of some of the experiments performed and the peak that appeared

Exp.	1	2	…	6	…	9	…	13	…	16
F1≡AZI	min	max	…	max	…	min	…	min	…	max
F2≡TET	min	min	…	min	…	min	…	min	…	max
F3≡AMPIC	min	min	…	max	…	min	…	max	…	max
F4≡PEN	min	min	…	min	…	max	…	max	…	max
I (µA)	0.498	9.951	…	12.470	…	2.376	…	6.796	…	12.990

the smallest. According to the equation, the two factors 'AZI' and 'PEN' exert a stronger positive influence compared to the others. The three-factor interactions consistently exhibit a negative effect, whereas the four-factor interaction remains positive, though with the smallest contribution. These findings demonstrate that ignoring interactions may lead to misinterpretation of antibiotic concentrations in real samples. However, terms with negligible magnitude relative to experimental variability and lower-order effects could be excluded. In our model, looking at the coefficients, the following terms are negligible: −0.00035 × AMPIC × PEN; −0.00021 × AZI × TET × AMPIC; + 0.00025 × AZI × TET × AMIPC × PEN. The reduced model retained all main effects and only those interactions that materially altered the response surface. Dropping these terms, their influence is absorbed into the intercept, with no practical loss in predictive ability within the design region (5–20 μM for each factor). Consequently, the reduced model could be presented:

$$I^* = 0.719 \times AZI + 0.628 \times TET + 0.755 \times AMPIC + 0.032 \times PEN - 0.015 \times AZI \times TET - 0.016 \times AZI \times AMPIC + 0.035 \times AZI \times PEN - 0.023 \times TET \times AMPIC + 0.013 \times TET \times PEN - 0.0032 \times AZI \times TET \times PEN - 0.0022 \times AZI \times AMPIC \times PEN - 0.0016 \times TET \times AMPIC \times PEN - 9.269 \quad (4)$$

Application to real samples

In real matrices, the practical applicability of the CPE_ZnO sensor was evaluated using the standard addition method. Three river water samples form Albanian`s rivers, were selected to investigate potential matrix effects. To mitigate matrix interferences and ensure analytical reliability, the samples were diluted 1:1 with 0.2 M acetate buffer at pH~5. Subsequently, aliquots of AZI at concentrations of 4, 10, and 20 μM were spiked into the samples, and they were calculated corresponding recoveries. The results summarized in Table 4, obtained for the CPE_ZnO sensor in river water matrices demonstrate adequate analytical performance with moderate accuracy and precision, and matrix's tolerance. For River 1, the recoveries show a noticeable deviation at the lowest (75%) and intermediate (120%) spike levels, suggesting the presence of matrix effects, including possible signal suppression at low concentration and enhancement at intermediate concentration. The relatively high RSD at 4 μM (23.8%) further indicates reduced precision near the lower concentration range, likely due to proximity to the detection limit and increased susceptibility to matrix variability. In contrast, the low RSD at 20 μM (0.4%) reflects excellent repeatability at higher analyte levels. River 2 exhibits improved overall performance, with recoveries between 75% and 110% and consistently moderate precision (RSD ≤ 11.5%). The near-quantitative recovery at higher concentrations indicates that matrix effects are less pronounced in this sample, supporting the robustness of the method under varying environmental conditions. River 3 shows the most reliable analytical behavior, with recoveries consistently at or very close to 100% across all spike levels and acceptable RSD values (4.6–10.9%). This indicates negligible matrix interference and confirms the high accuracy and stability of the sensor response in this matrix. Variations in recovery values among river samples indicate the presence of matrix effects, likely

Table 4. Analytical performance of CPE_ZnO sensor in river water samples

No. River	AZI spiked (μM)	AZI found (μM)	Recovery (%)	RSD (%)
River 1	0	ND	-	-
	4	3	75	23.8
	10	12	120	12.8
	20	19	95	0.4
River 2	0	ND	-	-
	4	3	75	11.5
	10	11	110	3.7
	20	20	100	3.4
River 3	0	ND	-	-
	4	4	100	10.9
	10	10	100	4.6
	20	20	100	6.3

caused by coexisting inorganic ions and natural organic matter that influence adsorption processes and electron-transfer kinetics at the electrode interface. Signal suppression or enhancement observed at certain concentration levels suggests that matrix constituents may alter the local electrochemical environment and affect AZI oxidation efficiency.

Overall, these findings confirm that the CPE_ZnO sensor is suitable for the determination of AZI in environmental water samples, demonstrating good accuracy, acceptable precision, and satisfactory resistance to matrix effects, particularly at higher concentration levels. These performance characteristics are consistent with those reported for similar carbon-based electrochemical sensors for antibiotic detection in environmental matrices.

CONCLUSIONS

The application of alternative electrochemical methods that are simple, rapid, and low-cost provides valuable preliminary insights into the detection and analysis of various pollutants. In this study, modification of approximately 10% of the carbon paste with ZnO significantly enhanced the electrochemical performance of the electrode for azithromycin determination, improving both sensitivity and signal stability.

The factorial design approach provided comprehensive quantitative information, allowing a detailed evaluation of the influence of each experimental factor on the measured analytical signal. Importantly, this methodology enabled the assessment not only of the individual effects of the studied factors but also of their interactions. Among the main effects, all factors contributed positively to the signal, with AMPIC exhibiting the largest influence and PEN the smallest. Analysis of the interaction terms revealed that three-factor interactions consistently exerted a negative effect, whereas the four-factor interaction was positive, albeit minimal. Furthermore, the values predicted by the regression models (R^2=0.99999), both with coded and real variables, closely matched the experimental measurements, demonstrating the robustness and accuracy of the model in describing the system. Notably, the two factors AZI and PEN exhibited the strongest positive contributions to the analytical response compared to the other factors, highlighting their critical role in the overall electrochemical behavior. Compared with conventional univariate optimization approaches, the proposed methodology reduces experimental effort while providing more comprehensive information about factor interactions and analytical response behavior. The combination of ZnO-modified carbon paste electrodes and factorial analysis therefore represents a practical and versatile platform for electrochemical sensing applications. Although the proposed approach demonstrated satisfactory analytical performance, further investigation using a broader range of environmental samples would strengthen the evaluation of matrix effects under diverse real-world conditions.

Acknowledgments

The authors acknowledge support from the Academy of Sciences of Albania, the SUSNANO project (Grant Agreement No. 101059266), and the Institut Català de Nanociència i Nanotecnologia (ICN2), Barcelona, Spain, for assistance with SEM and EDXS characterizations.

REFERENCES

1. Ameda, A., Kulla, L., Shehu, A., Baraj, B., Cenolli, S., Broli, N., Vasjari, M. (available online). A new rGO@Ni nanocomposite for simultaneous detection of Pb(II) and Cd(II). *Sensing and Biosensing Research, 51*. https://doi.org/10.1016/j.sbsr.2026.100951
2. Awad, Y., Kim, S., Abd El-Azeem, S., Kim, K., Kim, K, Kim, K, Jeon, Ch, Lee, S., Sik Ok, Y. (2013). Veterinary antibiotics contamination in water, sediment, and soil near a swine manure composting facility. *Environmental Earth Sciences*, 1433–1440. https://doi.org/10.1007/s12665-013-2548-z
3. Belcovici, A., Ioana, Fort C., Elena, Mureşan L., Perhaiţa, J., Borodi, G., Liana Turdean, G. (2023). Zinc oxide nanostructured platform for electrochemical detection of heavy metals. *Electroanalysis, 35*(5). https://doi.org/10.1002/elan.202200395
4. Bentler, P., Leeuw, J. (2011). Factor analysis via components analysis. *Psychometrika., 76*(3), 461-470. https://doi.org/10.1007/s11336-011-9217-5
5. Bozo, S., Capparelli, E., Pojani, E. (2024). A cross-sectional analysis of antibiotic use: Attitudes and practices in the Albanian community. *Clinical Epidemiology and Global Health, 28*. https://doi.org/10.1016/j.cegh.2024.101658
6. Bruyndonckx, R., Adriaenssens, N., Versporten, A., Hens, N., Monnet, D., Molenberghs, G., Goossens, H., Weist, K., Coenen, S., the ESAC-Net study group. (2021). Consumption of antibiotics in the

community, European Union/European Economic Area, 1997–2017: data collection, management and analysis. *Journal of Antimicrobial Chemotherapy, 76*(2), ii2–ii6. https://doi.org/10.1093/jac/dkab171

7. C. Mohan, A., Renjanadevi, B. (2016). Preparation of zinc oxide nanoparticles and its characterization using scanning electron microscopy (SEM) and x-ray diffraction(XRD). *Procedia Technology, 24*, 761–766. https://doi.org/10.1016/j.protcy.2016.05.078
8. Cabello, F. C. (2006). Heavy use of prophylactic antibiotics in aquaculture: a growing problem for human and animal health and for the environment. *Environmental Microbiology, 8*(7), 1137–1144. https://doi.org/10.1111/j.1462-2920.2006.01054.x
9. Cherian, T., Ragavendran, C., Vijayan, S., Kurien, S., J.G.M. Peijnenburg, W. (2023). A review on the fate, human health and environmental impacts, as well as regulation of antibiotics used in aquaculture. *Environmental Advances*. (13)100411. https://doi.org/10.1016/j.envadv.2023.100411
10. Choi, W., Lahiri, I., Seelaboyina, R., Soo Kang, Y. (2010). Synthesis of Graphene and Its Applications: A Review. *Critical Reviews in Solid State and Materials Sciences, 35*(1), 52–71. https://doi.org/10.1080/10408430903505036
11. Chukwuka Okocha, R., Olufemi Olatoye, I., Bolarinwa Adedeji, O. (2018). Food safety impacts of antimicrobial use and their residues in aquaculture. *Public Health Reviews, 39*. https://doi.org/10.1186/s40985-018-0099-2
12. Ensafi, A., Allafchian, A., Rezaei, B. (2013). A sensitive and selective voltammetric sensor based on multiwall carbon nanotubes decorated with $MgCr_2O_4$ for the determination of azithromycin. *Colloids and Surfaces B: Biointerfaces, 103*, 468–474. https://doi.org/10.1016/j.colsurfb.2012.11.021
13. Fabregat-Safont, D., Gracia-Marín, E., Ibáñez, M., Pitarch, E., Hernández, F. (2023). Analytical key issues and challenges in the LC-MS/MS determination of antibiotics in wastewater. *Analytica Chimica Acta, 1239*. https://doi.org/10.1016/j.aca.2022.340739
14. Hoxha, I., Malaj, A., Malaj, L. (2015). Antibiotic use in Albania between 2011 and 2012. *The Journal of Infection in Developing Countries, 9*, 94–98.
15. Hu, L., Zhou, T., Feng, J., Jin, H., Tao, J., Luo, D., Mei, S., Yong-Ill, Lee. (2018). A rapid and sensitive molecularly imprinted electrochemiluminescence sensor for Azithromycin determination in biological samples. *Journal of Electroanalytical Chemistry, 813*, 1–8. https://doi.org/10.1016/j.jelechem.2018.02.010
16. Kołodziejczak-Radzimska, A., Jesionowski, T.. (2014). Zinc oxide—from synthesis to application: A review. *Materials, 7*(4), 2833–2881. https://doi.org/10.3390/ma7042833
17. Kulla, L., Ameda, A., Jakubec, P., Baraj, B., Shehu, A., Cenolli, S., Broli, N., Vasjari, M., Otyepka, M. (available online). Factorial design-assisted simultaneous electrochemical sensing of neonicotinoid pesticides using a Ni-rGO-modified electrode. *Sensing and Biosensing Research, 51*. https://doi.org/10.1016/j.sbsr.2026.100992
18. Kumar, A., Pal, Dh. (2018). Antibiotic resistance and wastewater: Correlation, impact and critical human health challenges. *Journal of Environmental Chemical Engineering, 6*(1), 52–58. https://doi.org/10.1016/j.jece.2017.11.059
19. Liu, Y., Chen, J., Hu, H., Qu, K., Cui, Zh. (2022). A low-cost electrochemical method for the determination of sulfadiazine in aquaculture wastewater. *International Journal of Environmental Research and Public Health, 19*(24). https://doi.org/10.3390/ijerph192416945
20. Lowdon, J., Diliën, H., Singla, P., Peeters, M., Cleij, T., Grinsven, B., Eersels, K. (2020). MIPs for commercial application in low-cost sensors and assays – An overview of the current status quo,. *Sensors and Actuators B: Chemical, 325*. https://doi.org/10.1016/j.snb.2020.128973
21. Machowska, A., Stålsby Lundborg, C. (2018). Drivers of irrational use of antibiotics in Europe. *International journal of environmental research and public health, 16*. https://doi.org/10.3390/ijerph16010027
22. Mihani, J., Këlliçi, S.. (2018). Patterns of antibiotic prescription in children: Tirana, Albania Region. *Macedonian Journal of Medical Sciences, 6*(4), 719–722.
23. Mishra, S., Kumar Singh, A., Cheng, L., Hussain, A., Maiti, A. (2023). Occurrence of antibiotics in wastewater: Potential ecological risk and removal through anaerobic–aerobic systems. *Environmental Research*. https://doi.org/10.1016/j.envres.2023.115678
24. Mohd Noor, N., Kamaruzaman, N., Al-Gheethi, A., Radin Mohamed, R., Hossain, S. (2023). Degradation of antibiotics in aquaculture wastewater by bio-nanoparticles: A critical review. *Ain Shams Engineering Journal*. https://doi.org/10.1016/j.asej.2022.101981
25. Mohsen, Tavakol., Angela, Wetzel. (2020). Factor Analysis: a means for theory and instrument development in support of construct validity. *International Journal of Medical Education, 11*, 245–247.
26. Muaz, K., Riaz, M., Akhtar, S., Park, S., Ismail, A. (2018). Antibiotic residues in chicken meat: Global prevalence, threats, and decontamination strategies: A review. *Journal of Food Protection, 81*(4), 619–627. https://doi.org/10.4315/0362-028X.JFP-17-086
27. Nguyen, V., George Ayankojo, A., Reut, J., Rappich, J., Furchner, A., Hinrichs, K., Syritski, V. (2023). Molecularly imprinted co-polymer for class-selective electrochemical detection of macrolide antibiotics in

aqueous media. *Sensors and Actuators B: Chemical, 374*. https://doi.org/10.1016/j.snb.2022.132768

28. Novakovic, Z., Vasiljevic, Z., Vesna, Nikolic, M., Tadic, N., Djordjevic, T., Radovic, M., Gadjanski, I., Papović, S., Vlahovic, F., Stankovic, D., Vidic, J. (2025). ZnO-nanostructured electrochemical sensor for efficient detection of glyphosate in water. *Talanta Open, 12*. https://doi.org/10.1016/j.talo.2025.100481
29. Pan, Y., Shan, D., Ding, L., Yang, L., Xu,, K., Huang, H., Wang J., Ren, H. (2021). Developing a generally applicable electrochemical sensor for detecting macrolides in water with thiophene-based molecularly imprinted polymers. *Water Research, 205*. https://doi.org/10.1016/j.watres.2021.117670
30. Patil, VB., Ilager, D., Tuwar, SM., Mondal, K., Shetti, NP. (2022). Nanostructured ZnO-based electrochemical sensor with anionic surfactant for the electroanalysis of trimethoprim. *Bioengineering*, *9*(10):521. https://doi.org/10.3390/bioengineering9100521
31. Peng, J., Tao Hou, Ch., Xian Liu, X., Bo Li, H., Ya Hu, X. (2011). Electrochemical behavior of azithromycin at graphene and ionic liquid composite film modified electrode. *Talanta, 86*, 227–232. https://doi.org/10.1016/j.talanta.2011.09.005
32. Pogăcean, F., Varodi, C., Măgeruşan, L., Stefan-van Staden, R., Pruneanu, S. (2022). Highly sensitive electrochemical detection of azithromycin with graphene-modified electrode. *Sensors (Basel, Switzerland), 22*(16). https://doi.org/10.3390/s22166181
33. Schar, D., Klein, E., Laxminarayan, R., Gilbert, M., Van Boeckel, T. (2020). Global trends in antimicrobial use in aquaculture. *Scientific Reports, 10*, 21878. https://doi.org/10.1038/s41598-020-78849-3
34. Shrestha, N. (2021). Factor analysis as a tool for survey analysis. *American Journal of Applied Mathematics and Statistics, 9*, 4–11.
35. Souza, S., Junqueira, R., Ginn, R. (2005). Analysis of semicarbazide in baby food by liquid chromatography tandem mass spectrometry (LC–MS–MS)—In-house method validation. *Journal of Chromatography A, 1077*(2), 151–158. https://doi.org/10.1016/j.chroma.2005.04.062
36. Sulciute, A., Nishimura, K., Gilshtein, E., Cesano F., Viscardi, G., Nasibulin, A., Ohno, Y., Rackauskas, S. (2021). ZnO nanostructures application in electrochemistry: Influence of morphology. *The Journal of Physical Chemistry C, 125*(2). https://dx.doi.org/10.1021/acs.jpcc.0c08459
37. Sun, Q., Luo, J., Zhang, L., Zhang, Zh., Le, T. (2018). Development of monoclonal antibody-based ultrasensitive enzyme-linked immunosorbent assay and fluorescence-linked immunosorbent assay for 1-aminohydantoin detection in aquatic animals. *Journal of Pharmaceutical and Biomedical Analysis, 147*, 417–424. https://doi.org/10.1016/j.jpba.2017.06.068
38. Tavares, A, Helena de Sá, M., Goreti, Sales M. (2021). Innovative screen-printed electrodes on cork composite substrates applied to sulfadiazine electrochemical sensing. *Journal of Electroanalytical Chemistry, 880*. https://doi.org/10.1016/j.jelechem.2020.114922
39. Vajdle, O., Guzsvány, V., Škorić, D., Csanádi, J., Petković, M., Avramov-Ivić, M., Kónya, Z., Petrović, S., Bobrowski, A. (2017). Voltammetric behavior and determination of the macrolide antibiotics azithromycin, clarithromycin and roxithromycin at a renewable silver – amalgam film electrode. *Electrochimica Acta, 229*, 334–344. https://doi.org/10.1016/j.electacta.2017.01.146
40. Wang, Ch., Wang, Ch., Zhang, X., Ren, X., Yu, B., Wang, P., Zhao, Z., Fu, H. (2022). A new Eu-MOF for ratiometrically fluorescent detection toward quinolone antibiotics and selective detection toward tetracycline antibiotics. *Chinese Chemical Letters, 33*(3), 1353–1357. https://doi.org/10.1016/j.cclet.2021.08.095
41. Wang, M., Zheng, X., Yangcuo, Zh., Zhang, Sh, Xie, L., Cai, Q. (2024). A novel synchronous fluorescence spectrometry combined with fluorescence sensitization for the highly sensitive and simultaneous detection of enoxacin, ofloxacin and tetracycline hydrochloride residues in wastewater. *Talanta, 271*. https://doi.org/10.1016/j.talanta.2024.125707
42. Wang, Zh, Wang, X., Tian, H., Wei, Q., Liu, B., Bao, G., Liao, M., Peng, J., Huang, X., Wang, L. (2019). High through-put determination of 28 veterinary antibiotic residues in swine wastewater by one-step dispersive solid phase extraction sample cleanup coupled with ultra-performance liquid chromatography-tandem mass spectrometry. *Chemosphere, 230*, 337–346. https://doi.org/10.1016/j.chemosphere.2019.05.047
43. Yadav, M.S., Singh, N., Kumar, A. (2018). Synthesis and characterization of zinc oxide nanoparticles and activated charcoal based nanocomposite for supercapacitor electrode application. *J Mater Sci: Mater Electron* 29, 6853–6869. https://doi.org/10.1007/s10854-018-8672-5
44. Zaaba, N.I., Foo, K.L., Hashim, U., Tan, S.J., Liu, W., Voon, C.H. (2017). Synthesis of Graphene Oxide using Modified Hummers Method: Solvent Influence. *Procedia Engineering, 184*, 469–477. https://doi.org/10.1016/j.proeng.2017.04.118
45. Zokhtareh, R., Rahimnejad, M., Najafpour-Darzi, G., Karimi-Maleh, H. (2023). A novel sensing platform for electrochemical detection of metronidazole antibiotic based on green-synthesized magnetic Fe_3O_4 nanoparticles. *Environmental Research, 216*. https://doi.org/10.1016/j.envres.2022.114643